

Original Article

Asian Pacific Journal of Tropical Biomedicine

apjtb.org

doi: 10.4103/apjtb.apjtb_366_26

Cristazine inhibits HPV−positive cervical cancer cells *via* inducing caspase−dependent apoptosis

Mi Jeong Jo[1,2], Jeong Gyu Kim[1], Seung Hyun Yoo[1], Cha Young Kim[3], Jong−Oh Kim[1]✉, Gun−Do Kim[1]✉

[1]*Department of Microbiology, Pukyong National University, Busan 48513, Republic of Korea*

[2]*Institute of Sustainable Earth and Environment Dynamics, Pukyong National University, Busan, 48513, Republic of Korea*

[3]*Biological Resource Center, Korea Research Institute of Bioscience and Biotechnology, Jeongeup 56212, Republic of Korea*

ABSTRACT

Objective: To determine whether cristazine inhibits HPV-positive cervical cancer cells and to elucidate its underlying mechanisms.

Methods: HeLa cells were treated with varying concentrations of cristazine, and cell viability, intracellular ROS, apoptosis, and apoptosis-related gene and protein expression were assessed using WST-1, DCF-DA flow cytometry, Annexin V-FITC/PI staining, quantitative RT-PCR, and Western blotting. Additionally, CaSki and SiHa cells were evaluated in viability assays, with selected ROS and apoptosis measurements performed in CaSki cells.

Results: After 24 h of treatment, cristazine reduced HeLa cell viability with an IC_{50} of 0.223 μM and increased intracellular ROS and apoptotic populations. Caspase inhibition substantially restored viability and reduced apoptosis. Cristazine also increased *TP53*, *CDKN1A*, *BAX*, *BCL2*, and *CASP3* expression, and reduced HPV18 *E6*/*E7* expression. Additionally, Western blotting showed upregulated p53, p21 and Bax/Bcl-2 ratio, and increased cleavage of caspases-3, -8, -9, and -12 and PARP after cristazine treatment. DAPI staining showed chromatin condensation, while wound healing assays demonstrated reduced wound closure following cristazine treatment.

Conclusions: Cristazine suppresses cervical cancer cell growth *via* coordinated ROS-associated, p53-driven, and caspase-dependent apoptotic signaling, highlighting its potential as a marine-derived anticancer candidate that warrants further investigation.

KEYWORDS: Cristazine; Dioxopiperazine alkaloid; Apoptosis; HPV-positive cervical cancer; ROS; p53; *Chaetomium cristatum*

1. Introduction

Cancer involves uncontrolled cell cycle progression and evasion of apoptosis. Inducing apoptosis and blocking the cell cycle are promising strategies for cancer prevention and treatment[1]. Cervical cancer remains a major global health issue, with persistent infection by high-risk human papillomavirus (HPV) being a primary causative factor. Recent clinical and molecular studies highlight that HPV oncoproteins, particularly E6 and E7, play a significant role in disrupting tumor suppressor networks and cell cycle regulation[2−5]. Natural products are continuously being studied as potential sources of anticancer compounds, including substances that regulate apoptosis and oxidative stress[6−8]. Since the present study focused on a limited cell model and did not directly verify p53 phosphorylation or HPV dependence, these mechanisms should be interpreted as associations rather than established causal pathways.

Summary

Question: Does cristazine suppress HPV-positive cervical cancer cells and what is the underlying mechanism of its anti-proliferative action?

Findings: Cristazine inhibits cervical cancer cells by increasing ROS and promoting caspase-dependent apoptosis.

Meaning: Cristazine exerts anti-proliferative effects against cervical cancer cells by triggering caspase-dependent apoptosis, positioning it as a promising marine-derived lead compound for future therapeutic development.

✉To whom correspondence may be addressed. E-mail: jokim@pknu.ac.kr (JO. Kim); gundokim@pknu.ac.kr (GD. Kim)

This is an open access article distributed under the terms of the Creative Commons Attribution-Non-Commercial-No Derivatives License 4.0 (CCBY-NC-ND), where it is permissible to download and share the work provided it is properly cited. The work cannot be changed in any way or used commercially without permission from the journal.

For reprints contact: reprints@medknow.com

©2026 *Asian Pacific Journal of Tropical Biomedicine* Produced by Wolters Kluwer-Medknow.

How to cite this article: Jo MJ, Kim JG, Yoo SH, Kim CY, Kim JO, Kim GD. Cristazine inhibits HPV-positive cervical cancer cells *via* inducing caspase-dependent apoptosis. Asian Pac J Trop Biomed 2026; 16(12): 527-536.

Article history: Received 19 June 2026; Revision 5 August 2026; Accepted 7 September 2026; Available online 22 October 2026

Apoptosis, or programmed cell death, is critical for suppressing tumor growth and removing abnormal cells, and cancer cells often evade this process[9,10]. This evasion frequently involves abnormal caspase activity[10], which disrupts apoptosis[11]. Caspases are key for cancer development, progression, and therapy[11]. Reactive oxygen species (ROS) can act as signaling molecules, but increased concentrations can promote cellular stress and apoptosis[12,13]. Some anticancer drugs increase ROS to trigger oxidative stress in cancer cells[14]. Higher ROS levels are closely linked to caspase activation and apoptosis[13]. Regulating ROS is therefore important for cancer treatment.

Marine flora has long been used in medicine in regions such as India, China, and Europe, and seaweed has been part of diets in China and Japan since ancient times. Polyketides, made by bacteria, fungi, and plants, have diverse physiological activities and are potential drug candidates[15]. Marine fungi are known sources of structurally diverse secondary metabolites with biological activity[16,17]. *Chaetomium* sp. produces various bioactive metabolites, and cristazine is a dioxopiperazine alkaloid isolated from the mudflat-sediment-derived fungus *Chaetomium cristatum* (*C. cristatum*)[18]. Previous studies have shown that cristazine exhibits cytotoxic and apoptotic activity in A431 cancer cells[19,20], but the molecular responses associated with its effects on HPV-positive cervical cancer cells have not yet been fully elucidated. Accordingly, this study evaluated the effects of cristazine on cell viability and apoptosis of cervical cancer, focusing particularly on ROS accumulation, HPV18 E6/E7 expression, p53-related proteins, and caspase activation.

2. Methods

2.1. Sample preparation

Cristazine, previously isolated from *C. cristatum*, was kindly provided by Professor Son as a purified powder and stored at −80℃ until use[19]. In brief, *C. cristatum*, isolated from Suncheon Bay sediments, was cultured in seawater-based medium for three weeks. The culture was extracted with CH_2Cl_2-MeOH, and the crude extract was fractionated by silica gel and ODS chromatography. Final purification by HPLC afforded cristazine as a colorless solid. It was dissolved in dimethyl sulfoxide and diluted to the desired concentrations. The final dimethyl sulfoxide concentration was maintained below 0.1%.

2.2. Cell culture

The human cervical adenocarcinoma cell line HeLa was purchased from the American Type Culture Collection (VA, USA). CaSki and SiHa cervical carcinoma cell lines were obtained from the Korean Cell Line Bank (Seoul, Korea). HeLa and SiHa cells were cultured in Dulbecco's Modified Eagle's medium (Corning, NY, USA) supplemented with 10% fetal bovine serum (Corning, NY, USA) and 1% penicillin-streptomycin (Corning, NY, USA), whereas CaSki cells were maintained in RPMI 1640 medium. All cells were maintained at 37℃ in a humidified incubator with 5% CO_2. CaSki and SiHa cells were included in the initial viability comparison to determine whether the response to cristazine extended beyond HeLa cells; selected ROS and apoptosis assays were subsequently performed in CaSki cells, while detailed mechanistic analyses were focused on HeLa cells, which showed the clearest response.

2.3. Cell viability assay

HeLa cells were seeded at 1×10^5 cells/mL in a 96-well plate (SPL, Gyeonggi-do, Republic of Korea) and treated with various concentrations of cristazine (0-1.2 μM) for 12, 24 or 48 h. CaSki and SiHa cells were seeded under the same conditions and treated with varying concentrations of cristazine (0-1.2 μM) for 24 h. After treatment, the medium was replaced, and WST-1® reagent (Daeil Lab Service, Seoul, Republic of Korea) was added to each well. The cells were incubated for an additional 3 h, and absorbance was measured at 460 nm using an ELISA reader (Molecular Devices, San Jose, CA, USA). To assess caspase-dependent cell death, HeLa cells were co-treated with the Z-VAD-FMK (10 μM; V116; Sigma-Aldrich, St Louis, MO, USA), and cell viability was measured using the same method.

2.4. Flow cytometric analysis

HeLa and CaSki cells were plated in a 6-well plate and treated with cristazine (0.1 and 0.5 μM) for 24 h. Apoptosis was analyzed using the BD Pharmingen™ FITC Annexin V Apoptosis Detection Kit II (BD Biosciences, CA, USA) according to the manufacturer's instructions. To detect intracellular ROS, cells were stained with DCF-DA (Sigma-Aldrich) and analyzed as previously described[21]. Apoptotic populations and geometric mean ROS intensity were quantified using a BD FACSverse™ flow cytometer and analyzed with BD FACSuite™.

2.5. Western blotting

HeLa cells were cultured in a 100 mm dish (SPL) and treated with cristazine (0.1 and 0.5 μM) for 24 h. The cells were lysed using PRO-PREP protein extraction solution (iNtRON Biotechnology, Gyeonggi-do, Republic of Korea). Equal amounts of protein were separated using 12% SDS-PAGE (Bio-Rad, CA, USA) and electro-transferred onto a nitrocellulose membrane (PALL Life Sciences, Pensacola, FL, USA). The membranes were blocked with 5% skim milk in PBST and incubated overnight at 4℃ with primary antibodies. For Cell Signaling Technology antibodies, the catalog numbers and manufacturer-recommended Western blot dilutions were as follows: p53 (cat. no. 9282, 1∶1 000), p21 (cat. no. 2947, 1∶1 000), Bax (cat. no. 5023, 1∶1 000), Bcl-2 (cat. no.

2870, 1:1 000), cleaved caspase-8 (cat. no. 9496, 1:1 000), cleaved caspase-9 (cat. no. 20750, 1:1 000), cleaved caspase-3 (cat. no. 9661, 1:1 000), cleaved PARP (Asp214; cat. no. 5625, 1:1 000), DFF45/DFF35 (cat. no. 9732, 1:1 000), cleaved DFF45 (Asp224; cat. no. 9731, 1:1 000), GAPDH (cat. no. 2118, 1:1 000), and β-actin (cat. no. 4970, 1:1 000). Caspase-12 was detected using an Abcam antibody (cat. no. ab62484; 1:1 000). HRP-conjugated secondary antibodies were used according to the manufacturer's instructions. Detection was performed using Amersham ECL Advance Western Blotting Detection Kit and Hyperfilm ECL (GE Healthcare, Buckinghamshire, UK) or ChampChemi (Korea Lab Tech, Republic of Korea). Band intensities were quantified using ImageJ.

2.6. Quantitative real–time PCR (qRT–PCR)

HeLa cells were cultured in a 6-well plate and treated with cristazine (0.1 and 0.5 μM) for 24 h. Total RNA was extracted using the yesR™ Total RNA Extraction Kit (GenesGen, Busan, Republic of Korea), and 1 μg of RNA was reverse-transcribed using AccuPower® RT premix (Bioneer, Daejeon, Republic of Korea) under the following conditions: 42℃ for 1 h, 95℃ for 5 min, then held at 4℃. qRT-PCR was performed using the Prime Q-Master Mix with SYBR Green I (GenetBio, Daejeon, Republic of Korea) on a QuantStudio 6 Flex Real-Time PCR system (Thermo Fisher Scientific, Waltham, MA, USA). The primer sequences are listed in Supplementary Table[22]. The PCR cycling conditions were: 95℃ for 10 min; 40 cycles of 95℃ for 15 s, 60℃ for 30 s, 72℃ for 30 s; 95℃ for 15 s; followed by a melting curve analysis from 60℃ to 95℃. Gene expression was normalized to that of *GAPDH* using the comparative threshold cycle method ($2^{-\Delta\Delta CT}$).

2.7. DAPI staining

HeLa cells were cultured on coverglass-bottom dishes (SPL) with cristazine (0.1 and 0.5 μM) for 24 h. Then, the cells were treated with DAPI (Sigma-Aldrich) in MeOH for 15 min at 37℃, and then the cells were washed with 1 × PBS. Stained cells were mounted using ProLong™ Gold Antifade Mountant (Life Technologies, NY, USA) and observed under a Nikon ECLIPSE 50i microscope equipped with a CCD camera (Nikon, Tokyo, Japan). Images were captured and processed with High-Content Analysis Software (Cambridge Healthtech Ins., MA, USA).

2.8. Wound healing assay

HeLa cells were grown in a 6-well cell culture plate to 100% confluence. The confluent cells were carefully scratched with sterile tips, and any cellular debris was removed. The wounded monolayer was incubated in the presence of 0.1 and 0.5 μM of cristazine for 24 h.

2.9. Statistical analysis

Data are expressed as mean ± standard deviation (SD) from at least three independent experiments. Statistical analyses were conducted using one-way analysis of variance (ANOVA) with Dunnett's *post hoc* test or two-way ANOVA with Tukey's *post hoc* test using GraphPad Prism 9.0 (GraphPad, La Jolla, CA, USA). Differences were considered significant at $P < 0.05$.

3. Results

3.1. Cristazine inhibits cervical cancer cell proliferation

To evaluate the effect of cristazine on cervical cancer cell proliferation, a WST-1 assay was performed. HeLa cells were treated with different concentrations of cristazine for 24 h, and viability decreased in a concentration-dependent manner ($P < 0.05$ *vs.* control,

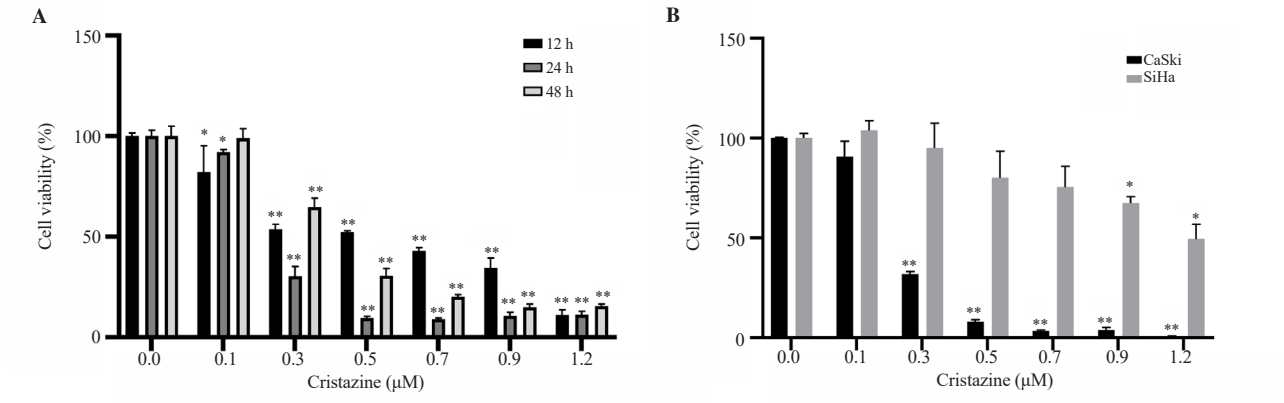


Figure 1. Cristazine reduces the viability of cervical cancer cells. (A) HeLa cells were treated with increasing concentrations of cristazine (0-1.2 μM) for 12-48 h. (B) CaSki and SiHa cells were treated with increasing concentrations of cristazine (0-1.2 μM) for 24 h. Cell viability was assessed using a WST-1 assay and expressed as the percentage of viable cells relative to untreated controls. Data are expressed as mean ± SD of three independent experiments performed in triplicate. $^{*}P < 0.05$, $^{**}P < 0.001$ *vs.* control.

Figure 1A). The IC_{50} of cristazine was 0.223 μM in HeLa cells. Similarly, the inhibitory response was also observed at 12 and 48 h (Figure 1). For comparison, the HPV16-positive cervical cancer CaSki and SiHa cells were used, and concentration-dependent inhibition was also observed in CaSki cells ($P < 0.001$ *vs.* control, Figure 1B). Based on these results, HeLa cells were used as the primary model for subsequent mechanism analysis, and CaSki cells were used for selective confirmation analysis.

To determine whether caspase activity is involved in the reduction of cell viability, HeLa cells were co-treated with cristazine and the pan-caspase inhibitor Z-VAD-FMK. Co-treatment with Z-VAD-FMK significantly increased cell viability compared to cristazine alone at 0.1 μM ($P < 0.05$) and 0.5 μM ($P < 0.001$). At 0.5 μM cristazine, cell viability was reduced to less than 10%, whereas co-treatment with Z-VAD-FMK increased viability to approximately 90% (Figure 2). These results support a substantial contribution of caspase activity to cristazine-associated cytotoxicity.

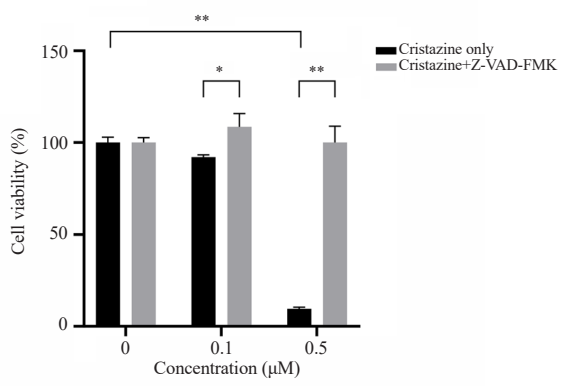


Figure 2. Caspase inhibition partially rescues cell viability. HeLa cells were treated with cristazine (0.1 or 0.5 μM) in the presence or absence of the pan-caspase inhibitor Z-VAD-FMK (10 μM) for 24 h. Cell viability was measured by WST-1 assay and is expressed as a percentage relative to the untreated control cells. Data are expressed as mean ± SD of three independent experiments. $^{*}P < 0.05$, $^{**}P < 0.001$.

3.2. Cristazine increases intracellular ROS levels in HeLa cells

To assess intracellular ROS, DCF-DA staining followed by flow cytometry was performed. Cristazine significantly increased ROS levels in HeLa cells in a concentration-dependent manner ($P < 0.001$ *vs.* control, Figure 3). A similar increase was observed in CaSki cells ($P < 0.001$ *vs.* control, Figure 4A). Because all measurements were performed 24 h after treatment, the results only demonstrate an association between cristazine exposure and ROS accumulation.

3.3. Cristazine modulates the expression of apoptosis-related genes

To identify transcriptional changes associated with cristazine treatment, apoptosis-related genes in HeLa cells were analyzed after 24 h (Figure 5). Cristazine increased the expression of *TP53*, *CDKN1A*, *BAX*, *BCL2*, and *CASP3*, although the magnitude of these changes differed among the genes. Cristazine also decreased the expression of HPV18 *E6*/*E7*. These coordinated changes are consistent with a shift toward a pro-apoptotic transcriptional profile. However, because additional p53 target genes such as PUMA and NOXA and p53 phosphorylation were not assessed in this study, these transcriptional changes cannot be taken as definitive evidence of p53 pathway activation.

3.4. Cristazine induces caspase-dependent apoptosis and inhibits cell migration

To determine whether cristazine-induced cell death was associated with apoptosis, Annexin V-FITC/PI staining and Western blotting were performed on HeLa cells (Figures 6 and 7). Treatment with 0.5 μM cristazine increased early and late apoptotic populations to 27.85% and 22.74%, respectively, compared with 3.46% and 9.85% in control cells. Z-VAD-FMK reduced the early and late

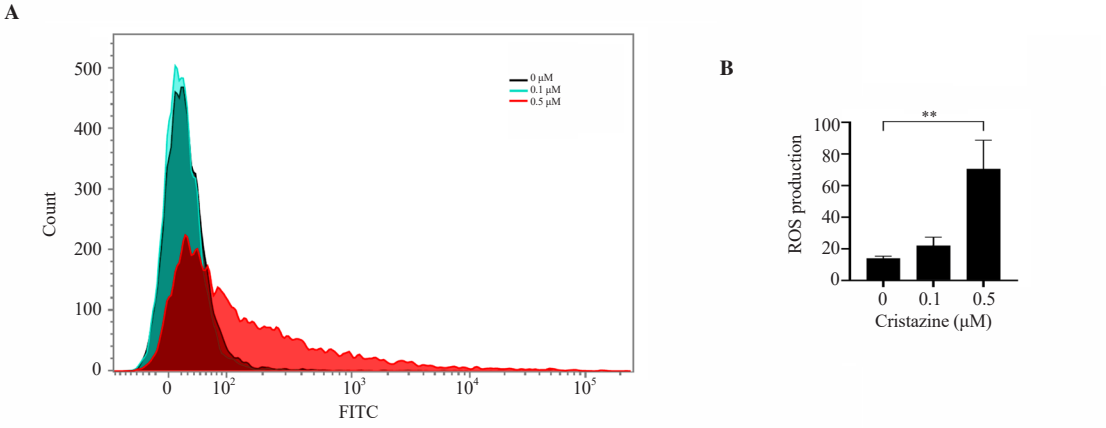


Figure 3. Cristazine increases intracellular reactive oxygen species (ROS) levels. (A) HeLa cells were incubated with cristazine (0.1 or 0.5 μM) for 24 h, then stained with dichlorodihydrofluorescein diacetate (DCF-DA). Intracellular ROS levels were quantified using flow cytometry. (B) Bars represent mean ± SD of three independent experiments. $^{**}P < 0.001$ *vs.* control.

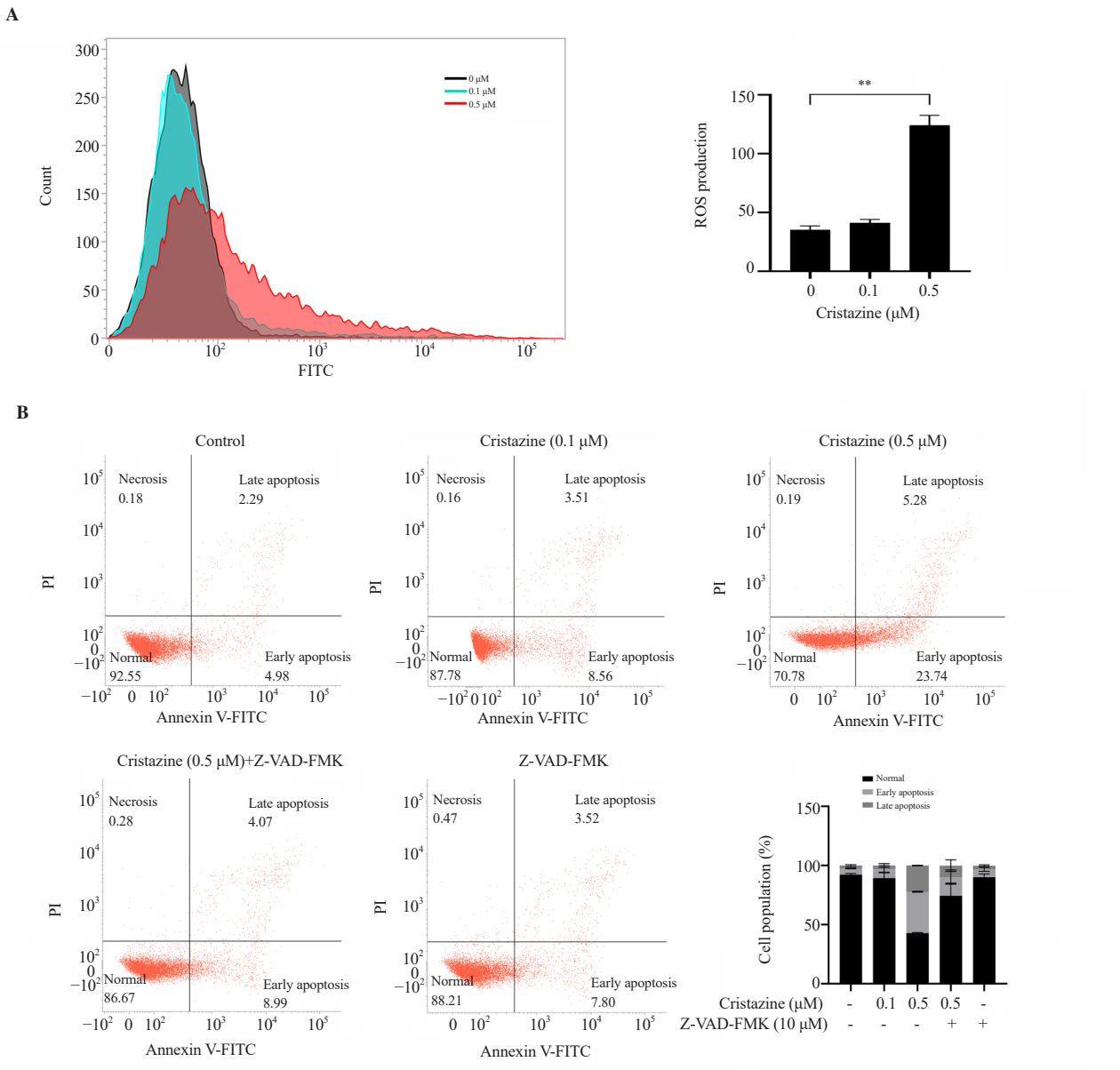


Figure 4. Cristazine regulates intracellular ROS levels and caspase-related apoptosis in CaSki cells. (A) CaSki cells were incubated with cristazine (0.1 or 0.5 μM) for 24 h, then stained with DCF-DA. Intracellular ROS levels were quantified using flow cytometry. Data are presented as mean ± SD of three independent experiments. $^{**}P < 0.001$ *vs.* control. (B) Annexin V-FITC/PI staining of CaSki cells treated with cristazine (0.1 or 0.5 μM) for 24 h in the presence or absence of Z-VAD-FMK (10 μM).

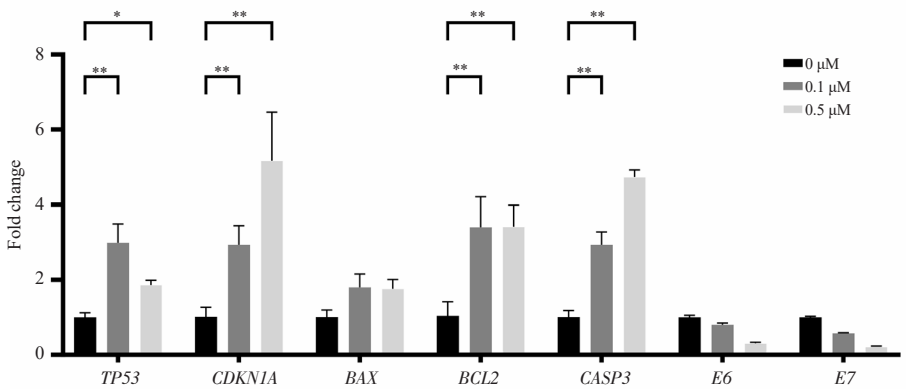


Figure 5. Cristazine regulates apoptosis-related gene expression. HeLa cells were treated with cristazine (0.1 or 0.5 μM) for 24 h. Total RNA was extracted and analyzed *via* quantitative real-time PCR. The mRNA levels of the indicated genes [*TP53*, *CDKN1A* (*p21*), *BAX*, *BCL2*, *CASP3*, and HPV *E6*/*E7*] were normalized to those of *GAPDH* and are expressed as fold change relative to the untreated cells. Bars represent mean ± SD of three independent experiments. $^{*}P < 0.05$, $^{**}P < 0.001$.

apoptotic populations to 3.30% and 9.16%, respectively, supporting a significant caspase-dependent component. CaSki cells also showed a similar apoptosis-associated response in the selected assays (Figure 4B). Western blotting showed that cristazine treatment increased cleavage of caspases-3, -8, -9, and -12. The expression levels of p53, cleaved PARP, and cleaved DFF45 were also upregulated (Figure 7). Moreover, cristazine treatment increased Bax protein expression, whereas Bcl-2 protein levels remained relatively unchanged at 0.1 μM and decreased at 0.5 μM cristazine. Accordingly, the Bax/Bcl-2 ratio was increased in a concentration-dependent manner, from 0.195

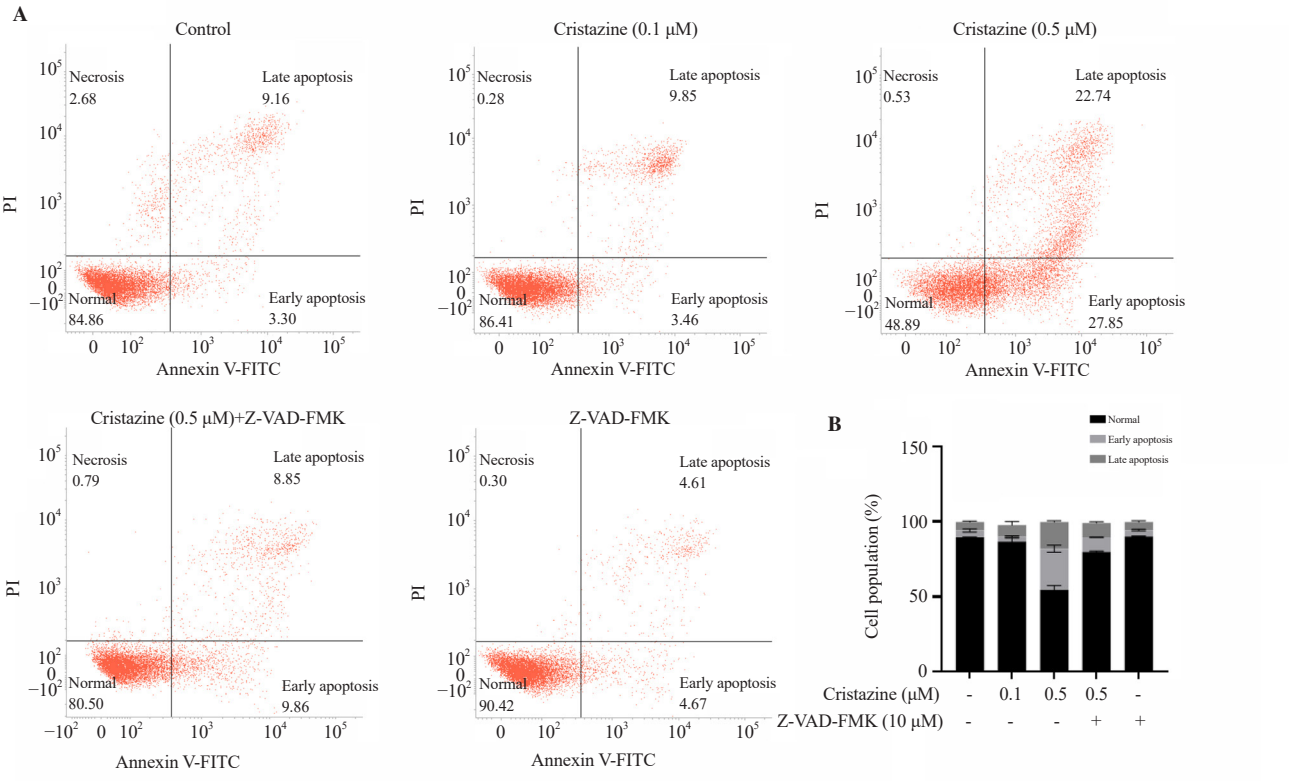


Figure 6. Cristazine induces apoptosis in HeLa cells. (A) Annexin V-FITC/PI staining of HeLa cells treated with cristazine (0.1 or 0.5 μM) for 24 h. (B) Representative graph showing populations of normal viable, early-apoptotic, and late-apoptotic cells. Cells were treated with cristazine in the presence or absence of Z-VAD-FMK (10 μM).

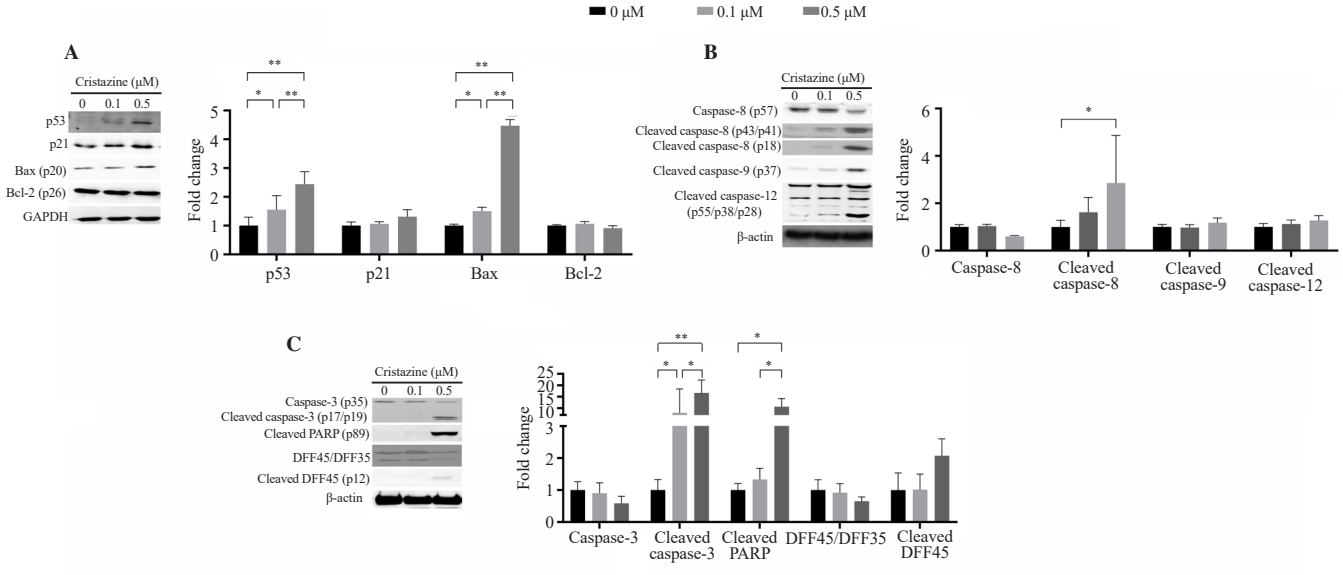


Figure 7. Cristazine regulates apoptosis-related protein. (A-C) Western blot analysis of HeLa cells treated with cristazine (0.1 or 0.5 μM) for 24 h. GAPDH or β-actin served as a loading control. Bar graphs are presented as mean ± SD of three independent experiments. $^{*}P < 0.05$, $^{**}P < 0.001$.

in control cells to 0.274 and 0.958 following treatment with 0.1 and 0.5 μM cristazine, respectively. The significant increase in the Bax/Bcl-2 ratio coincides with a transition to a cell death-promoting balance. Nuclear changes were observed *via* DAPI staining under a microscope. As the concentration of cristazine increased, the nucleus shrunk and chromatin was condensed. To investigate the effect of cristazine on HeLa cell motility, a wound-healing assay was performed. Compared with the control group, cristazine treatment significantly reduced wound healing ($P < 0.05$, Figure 8).

4. Discussion

This study shows that cristazine, a dioxopiperazine alkaloid derived from *C. cristatum*, exerts potent anticancer activity against HPV18-positive cervical cancer HeLa cells. Cristazine reduced cell viability in a concentration-dependent manner, with an IC_{50} of 0.223 μM at 24 h, and induced a pronounced apoptotic response. The involvement of caspases was demonstrated by the significant recovery of cell viability and reduction of apoptotic populations following treatment with the pan-caspase inhibitor Z-VAD-FMK. These results were further supported by increased cleavage of caspases-3, -8, -9, and -12 and PARP. These converging results indicate that caspase-dependent apoptosis is a major mechanism underlying cristazine-induced cytotoxicity in HeLa cells.

Cristazine also markedly increased intracellular ROS levels in HeLa cells, and a similar increase was observed in CaSki cells. Excessive ROS accumulation can promote cancer cell death through oxidative damage and activation of apoptotic signaling[12–14,23–25]. In the present study, ROS elevation occurred alongside increased apoptosis and the activation of various caspases, which supports the close association between oxidative stress and the apoptotic response to cristazine. ROS can also interact with p53-p21 signaling, which is relevant to the simultaneous increase of *TP53* and *CDKN1A* observed after cristazine treatment[12,26–29]. Thus, these findings suggest that ROS-related signaling is involved in cristazine-induced apoptosis, while the precise upstream mechanism of ROS needs to be elucidated through further research.

A particularly important finding is that the Bax/Bcl-2 ratio increased in a concentration-dependent manner. The ratio of protein expression increased from 0.195 in untreated cells to 0.274 and 0.958 following treatment with 0.1 and 0.5 μM cristazine, respectively. Interestingly, Bax and Bcl-2 showed different patterns at the mRNA and protein levels. Although cristazine treatment upregulated both *Bax* and *Bcl–2* mRNA transcription, the latter showed a more pronounced increase. In contrast, Western blot analysis demonstrated increased Bax protein expression, whereas Bcl-2 protein levels remained relatively unchanged. Consequently, the Bax/Bcl-2 protein ratio

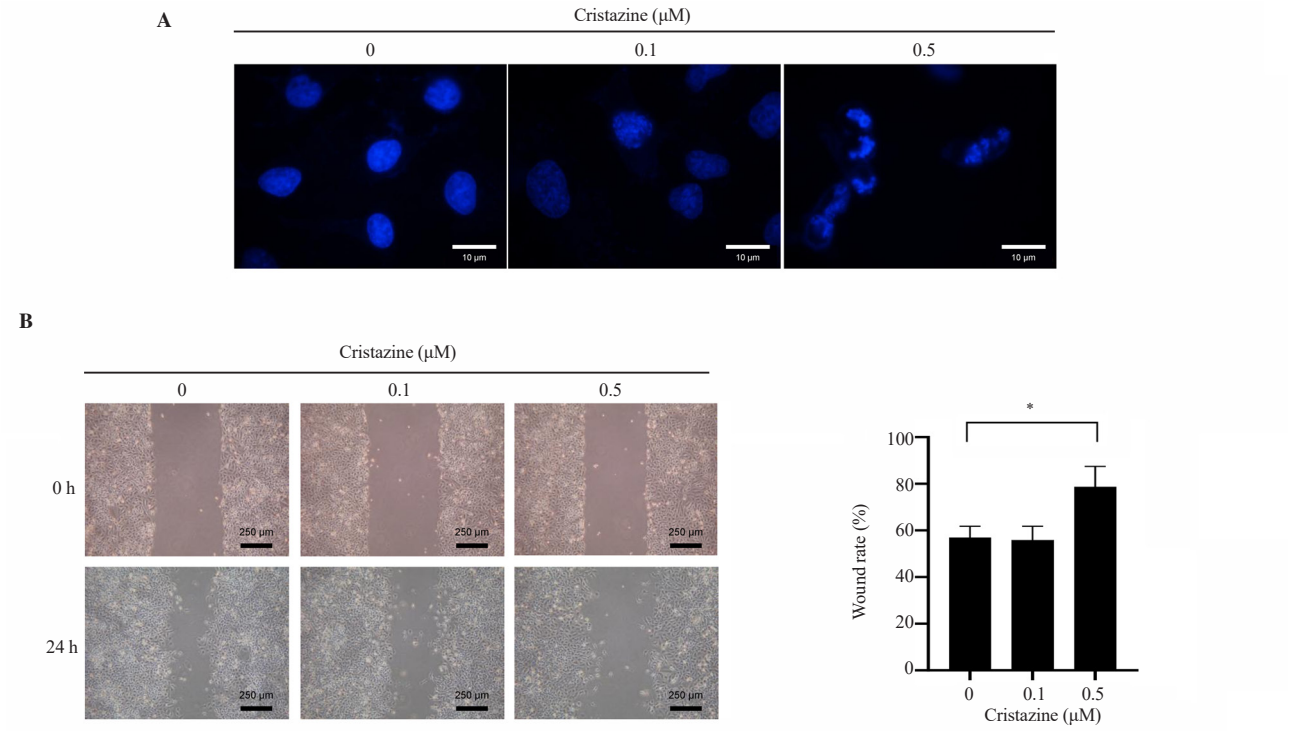


Figure 8. Effects of cristazine on chromatin condensation and wound closure. (A) HeLa cells were treated with cristazine (0.1 or 0.5 μM) for 24 h, stained with DAPI, and observed under an immunofluorescence microscope (×1 000 magnification). (B) HeLa cells were scratched and cultured with cristazine (0.1 or 0.5 μM) for 24 h and photographed under an inverted microscope (×40 magnification). The wound rate at 24 h is presented as mean ± SD of three independent experiments. $^{*}P < 0.05$.

shifted toward a pro-apoptotic balance. This discrepancy between transcript and protein levels may reflect post-transcriptional or post-translational regulation of Bcl-2. Since Bax promotes mitochondrial outer membrane permeability, while Bcl-2 acts as an anti-apoptotic regulator, this increase indicates a clear shift toward promoting apoptosis. This interpretation aligns with the increased activation of caspase-9 and caspase-3 and PARP cleavage. In addition, the activation of caspase-8 and caspase-12 suggests that cristazine is involved in multiple apoptotic signaling pathways[30–32]. The agreement between the Bax/Bcl-2 ratio, Annexin V/PI staining, Z-VAD-FMK inhibition, and apoptotic protein cleavage provides strong evidence for a potent caspase-dependent apoptotic response.

These findings further implicate p53-related signaling in the response to cristazine. Cristazine increased *TP53*, *CDKN1A* (*p21*) and *BAX* expression, and reduced HPV18 *E6* and *E7* expression. HPV E6 promotes p53 degradation through the E6-E6AP ubiquitin-proteasome pathway, thereby suppressing p53-dependent tumor-suppressor functions[6,33,34]. Accordingly, the decrease in HPV18 E6 expression together with increased total p53 and p21 is consistent with attenuation of HPV-related p53-related signaling inhibition. The coordinated changes in E6/E7, p53, p21, Bax, and Bcl-2 provide a consistent molecular framework for the apoptotic phenotype observed after cristazine treatment.

Although the present data support involvement of p53-related signaling, phospho-p53 (Ser15) was not measured; therefore, the increase in total p53 and p21 cannot be interpreted as direct evidence of p53 activation *via* Ser15 phosphorylation. Similarly, PUMA and NOXA were not investigated; however, the increase in the Bax/Bcl-2 ratio and the activation of caspase-9 and caspase-3 provide functional evidence for mitochondrial apoptotic signaling. Future studies incorporating analysis of p53 phosphorylation and additional p53 target genes will further elucidate the molecular pathways linking cristazine treatment to apoptosis execution.

The reduction of HPV18 E6/E7 expression is particularly relevant to the biological characteristics of HPV-associated cervical cancer. Natural compounds such as curcumin, epigallocatechin gallate, resveratrol, and berberine have been reported to suppress HPV oncogene expression and influence tumor-suppressor signaling in cervical cancer models[35–38]. The ability of cristazine to induce ROS production, shift the Bax/Bcl-2 balance toward pro-apoptosis, and trigger caspase-dependent cell death—even at low concentrations in HeLa cells—collectively supports its further exploration as a potential therapeutic agent against HPV-driven cervical cancer.

CaSki and SiHa cells were included in the viability analysis to determine whether the growth-inhibitory effect observed in HeLa cells also occurred in other HPV-positive cervical cancer cell lines. The subsequent mechanistic analyses were focused on HeLa because it showed the clearest and most consistent response, allowing for the detailed characterization of ROS generation, apoptosis, gene expression, and apoptotic protein activation. CaSki also showed increased ROS and an apoptotic response, supporting the relevance of cristazine activity beyond a single cell line. In contrast, the weaker response in SiHa suggests that cellular environment influences sensitivity to cristazine. Differences in HPV genotype, viral copy number or integration, and basal signaling networks may contribute to these differences and further research is required[39,40].

An HPV-negative cervical cancer model would provide an additional criterion for determining whether the response to cristazine is influenced by the HPV-associated molecular environment. Although this study did not include HPV-negative models, the current results establish potent anticancer and apoptotic effects in HPV-positive cervical cancer models and show simultaneous changes in HPV18 E6/E7 and p53-related signaling in HeLa cells. Future comparisons with HPV-negative models will help determine whether HPV status and cytogenetic background modulate cristazine sensitivity.

The Annexin V-FITC/PI results further support the finding that the primary mechanism of cristazine-induced cell death is apoptosis. The small Annexin V^-/PI^+ population in untreated control cells, which represents baseline necrosis or spontaneous cell death, appeared only infrequently and was not considered as treatment-induced necrosis. Cristazine increased both early and late apoptotic populations, whereas Z-VAD-FMK markedly reduced these populations. A proportion of PI-positive cells was also present in untreated control cells, which may reflect basal non-viable cells or cell damage incurred during sample preparation. The key observation was the increase in the number of apoptotic cells upon cristazine treatment, which was abrogated following caspase inhibition. Together with the molecular findings, these results support apoptosis rather than nonspecific loss of cell integrity as a major mechanism of cristazine-induced cytotoxicity.

Collectively, our results showed that cristazine induces apoptosis in HPV18-positive HeLa cells *via* ROS-mediated repression of viral oncogenes and reactivation of p53-driven apoptotic signaling. However, whether ROS directly targets HPV18 E6/E7 transcription or acts through upstream redox-sensitive regulators remains an open question. Addressing this, along with comparative studies in HPV-negative models, will be critical to delineate the HPV-specific contribution. Nevertheless, the present findings establish cristazine as a marine-derived compound with translational potential against HPV-associated cervical cancer.

Conflict of interest statement

The authors declare no competing interests.

Acknowledgments

We would like to express our gratitude to Byeng Wha Son, retired from the Department of Chemistry at Pukyong National University, for providing us with cristazine.

Funding

This research was supported by Global-Learning & Academic research institution for Master's PhD students, and Postdocs Program of the National Research Foundation of Korea grant funded by the Ministry of Education (No. RS-2023-00301702) and the Korean Research Institute of Bioscience and Biotechnology Research Initiative Program (KGM5282432).

Data availability statement

The data supporting the findings of this study are available from the corresponding authors upon request.

Declaration of generative AI and AI–assisted technologies in the manuscript preparation process

During the preparation of this work, the authors used ChatGPT and Grammarly in order to translate and edit the manuscript from Korean to English. After using this tool, the authors reviewed and edited the content as needed and took full responsibility for the publication's content.

Authors' contributions

MJJ contributed to the conceptualization, data curation, formal analysis, investigation, and writing of the original draft. JGK performed the formal analysis and software development and contributed to the review and editing of the manuscript. SHY contributed to the formal analysis and review and editing of the manuscript. CYK contributed to funding acquisition and review and editing of the manuscript. JOK contributed to funding acquisition and validation, and reviewed and edited the manuscript. GDK supervised the project and contributed to the review and editing of the manuscript. All authors have read and agreed to the published version of the manuscript.

References

[1] Matthews HK, Bertoli C, de Bruin RAM. Cell cycle control in cancer. *Nat Rev Mol Cell Biol* 2022; **23**(2): 74-88.

[2] Siegel RL, Kratzer TB, Giaquinto AN, Sung H, Jemal A. Cancer statistics, 2025. *CA Cancer J Clin* 2025; **75**(1): 10-45.

[3] Włoszek E, Krupa K, Skrok E, Budzik MP, Deptała A, Badowska-Kozakiewicz A. HPV and cervical cancer—Biology, prevention, and treatment updates. *Curr Oncol* 2025; **32**(3): 122. doi: 10.3390/curroncol32030122.

[4] Baba SK, Alblooshi SSE, Yaqoob R, Behl S, Al Saleem M, Rakha EA, et al. Human papilloma virus (HPV) mediated cancers: An insightful update. *J Transl Med* 2025; **23**(1). doi: 10.1186/s12967-025-06470-x.

[5] Janiszewska J, Kostrzewska-Poczekaj M, Wierzbicka M, Brenner J, Giefing M. HPV-driven oncogenesis—much more than the E6 and E7 oncoproteins. *J Appl Genet* 2025; **66**(1): 63-71.

[6] Chen Y, Yu D, Zhu D, Muthusamy S, Deshpande M, Kiruthiga N, et al. Exploring alkaloids and flavonoids from natural Sources: Emerging natural agents for inhibiting cervical cancer progression through apoptosis induction, anti-inflammatory effects, and oxidative stress reduction. *Pathol Res Pract* 2025. doi: 10.1016/j.prp.2025.156092.

[7] Gökalp F. The effective natural compounds for inhibiting cervical cancer. *Med Oncol* 2021; **38**(2). doi: 10.1007/s12032-021-01456-3.

[8] Chuerduangphui J, Loymunkong C, Ekalaksananan T, Pientong C. Arecoline, a main alkaloid in *Areca catechu*, induces biological changes in human papillomavirus 16-positive cervical cancer cells *via* upregulation of viral oncogenes and cellular transcriptional factors. *Asian Pac J Trop Biomed* 2025; **15**(3): 119-128.

[9] Carneiro BA, El-Deiry WS. Targeting apoptosis in cancer therapy. *Nat Rev Clin Oncol* 2020; **17**(7): 395-417.

[10]Kashyap D, Garg VK, Goel N. Intrinsic and extrinsic pathways of apoptosis: Role in cancer development and prognosis. *Adv Protein Chem Struct Biol* 2021; **125**: 73-120.

[11]Boice A, Bouchier-Hayes L. Targeting apoptotic caspases in cancer. *Biochim Biophys Acta Mol Cell Res* 2020; **1867**(6). doi: 10.1016/j.bbamcr.2020.118688.

[12]Cheung EC, Vousden KH. The role of ROS in tumour development and progression. *Nat Rev Cancer* 2022; **22**(5): 280-297.

[13]Nakamura H, Takada K. Reactive oxygen species in cancer: Current findings and future directions. *Cancer Sci* 2021; **112**(10): 3945-3952.

[14]Sarkar E, Kotiya A, Bhuyan R, Raza ST, Misra A, Ahmad R, et al. Curcumin chemo-sensitizes intrinsic apoptosis through ROS-mediated mitochondrial hyperpolarization and DNA damage in breast cancer cells. *Cell Signal* 2025; **128**. doi: 10.1016/j.cellsig.2025.111637.

[15]Evidente A. Advances on anticancer fungal metabolites: Sources, chemical and biological activities in the last decade (2012-2023). *Nat Prod Bioprospect* 2024; **14**. doi: 10.1007/s13659-024-00452-0.

[16]Gao Y, Wang J, Meesakul P, Zhou J, Liu J, Liu S, et al. Cytotoxic

compounds from marine fungi: Sources, structures, and bioactivity. *Mar Drugs* 2024; **22**(2): 70. doi: 10.3390/md22020070 .

[17]Noman E, Al-Shaibani MM, Bakhrebah MA, Almoheer R, Al-Sahari M, Al-Gheethi A, et al. Potential of anti-cancer activity of secondary metabolic products from marine fungi. *J Fungi (Basel)* 2021; **7**(6): 436. doi: 10.3390/jof7060436.

[18]Tian Y, Li Y. A review on bioactive compounds from marine-derived *Chaetomium* species. *J Microbiol Biotechnol* 2022; **32**(5): 541-550.

[19]Yun K, Khong TT, Leutou AS, Kim GD, Hong J, Lee CH, et al. Cristazine, a new cytotoxic dioxopiperazine alkaloid from the mudflat-sediment-derived fungus *Chaetomium cristatum*. *Chem Pharm Bull* 2016; **64**(1): 59-62.

[20]Jo MJ, Patil MP, Jung HI, Seo YB, Lim HK, Son BW, et al. Cristazine, a novel dioxopiperazine alkaloid, induces apoptosis *via* the death receptor pathway in A431 cells. *Drug Dev Res* 2019; **80**(4): 504-512.

[21]Eruslanov E, Kusmartsev S. Identification of ROS Using oxidized DCFDA and flow-cytometry. In: Armstrong D (ed.) *Advanced protocols in oxidative stress II. Methods in molecular biology*. Totowa, NJ: Humana Press; 2010, p. 57-72.

[22]Bordigoni A, Motte A, Tissot-Dupont H, Colson P, Desnues C. Development and validation of a multiplex qPCR assay for detection and relative quantification of HPV16 and HPV18 *E6* and *E7* oncogenes. *Sci Rep* 2021; **11**(1). doi: 10.1038/s41598-021-83489-2.

[23]Sarmiento-Salinas FL, Perez-Gonzalez A, Acosta-Casique A, Ix-Ballote A, Diaz A, Treviño S, et al. Reactive oxygen species: Role in carcinogenesis, cancer cell signaling and tumor progression. *Life Sci* 2021; **284**. doi: 10.1016/j.lfs.2021.119942.

[24]Shah MA, Rogoff HA. Implications of reactive oxygen species on cancer formation and its treatment. *Semin Oncol* 2021; **48**(3): 238-245.

[25]Glorieux C, Liu S, Trachootham D, Huang P. Targeting ROS in cancer: Rationale and strategies. *Nat Rev Drug Discov* 2024; **23**(8): 583-606.

[26]Koo N, Sharma AK, Narayan S. Therapeutics targeting p53-MDM2 interaction to induce cancer cell death. *Int J Mol Sci* 2022; **23**(9). doi: 10.3390/ijms23095005.

[27]Kung CP, Weber JD. It's getting complicated—A fresh look at p53-MDM2-ARF triangle in tumorigenesis and cancer therapy. *Front Cell Dev Biol* 2022; **10**. doi: 10.3389/fcell.2022.818744.

[28]Macip S, Igarashi M, Fang L, Chen A, Pan ZQ, Lee SW, et al. Inhibition of p21-mediated ROS accumulation can rescue p21-induced senescence. *EMBO J* 2002; **21**(9): 2180-2188.

[29]Masgras I, Carrera S, De Verdier PJ, Brennan P, Majid A, Makhtar W, et al. Reactive oxygen species and mitochondrial sensitivity to oxidative stress determine induction of cancer cell death by p21. *J Biol Chem* 2012; **287**(13): 9845-9854.

[30]Barez SR, Atar AM, Aghaei M. Mechanism of inositol-requiring enzyme 1-alpha inhibition in endoplasmic reticulum stress and apoptosis in ovarian cancer cells. *J Cell Commun Signal* 2020; **14**(4): 403-415.

[31]Wu H, Guo H, Liu H, Cui H, Fang J, Zuo Z, et al. Copper sulfate-induced endoplasmic reticulum stress promotes hepatic apoptosis by activating CHOP, JNK and caspase-12 signaling pathways. *Ecotoxicol Environ Saf* 2020; **191**. doi: 10.1016/j.ecoenv.2020.110236.

[32]Liu YN, Mu YD, Wang H, Zhang M, Shi YW, Mi G, et al. Endoplasmic reticulum stress pathway mediates T-2 toxin-induced chondrocyte apoptosis. *Toxicology* 2021; **464**. doi: 10.1016/j.tox.2021.152989.

[33]Scarth JA, Patterson MR, Morgan EL, Macdonald A. The human papillomavirus oncoproteins: A review of the host pathways targeted on the road to transformation. *J Gen Virol* 2021; **102**(3). doi: 10.1099/jgv.0.001540.

[34]Ranasinghe V, McMillan N. Novel therapeutic strategies for targeting E6 and E7 oncoproteins in cervical cancer. *Crit Rev Oncol Hematol* 2025; **211**. doi: 10.1016/j.critrevonc.2025.104721.

[35]Sadeghi RV, Parsania M, Sadeghizadeh M. Investigation of curcumin-loaded OA400 nanoparticle's effect on the expression of E6 and E7 human papilloma-virus oncogenes and P53 and Rb factors in HeLa cell line. *Iran J Pharm Res* 2022; **21**(1). doi: 10.5812/ijpr-130762.

[36]Pan M, Behmard V, Zare Z, Malekpour M, Nejadbiglari H, Yavari S, et al. Suppressing effects of green tea extract and epigallocatechin-3-gallate (EGCG) on TGF-β-induced epithelial-to-mesenchymal transition *via* ROS/Smad signaling in human cervical cancer cells. *Gene* 2021; **794**. doi: 10.1016/j.gene.2021.145774.

[37]Sun X, Fu P, Xie L, Chai S, Xu Q, Zeng L, et al. Resveratrol inhibits the progression of cervical cancer by suppressing the transcription and expression of HPV *E6* and *E7* genes. *Int J Mol Med* 2021; **47**(1): 335-345.

[38]Franconi R, Massa S, Paolini F, Vici P, Venuti A. Plant-derived natural compounds in genetic vaccination and therapy for HPV-associated cancers. *Cancers (Basel)* 2020; **12**(11). doi: 10.3390/cancers12113101.

[39]Qian S, Wei Z, Yang W, Huang J, Yang Y, Wang J. The role of BCL-2 family proteins in regulating apoptosis and cancer therapy. *Front Oncol* 2022; **12**. doi: 10.3389/fonc.2022.985363.

[40]Makgoo L, Mosebi S, Mbita ZA. Molecular mechanisms of HIV protease inhibitors against HPV-associated cervical cancer: Restoration of TP53 tumour suppressor activities. *Front Mol Biosci* 2022; **9**. doi: 10.3389/fmolb.2022.875208.

Publisher's note

The Publisher of the *Journal* remains neutral with regard to jurisdictional claims in published maps and institutional affiliations.

Edited by Liang Q, Tan BJ